Journal for ImmunoTherapy of Cancer

Neoadjuvant intratumoral influenza vaccine treatment in patients with proficient mismatch repair colorectal cancer leads to increased tumor infiltration of CD8+ T cells and upregulation of PD-L1: a phase 1/2 clinical trial

Mikail Gögenur ,[1] Lukas Balsevicius,[1] Mustafa Bulut,[1,2] Nesibe Colak,[1] Tobias Freyberg Justesen,[1] Anne-Marie Kanstrup Fiehn,[2,3] Marianne Bøgevang Jensen,[3] Kathrine Høst-Rasmussen,[1] Britt Cappelen,[1] Shruti Gaggar,[1] Asma Tajik,[1] Jawad Ahmad Zahid,[1] Astrid Louise Bjørn Bennedsen,[1] Tommaso Del Buono D'Ondes,[1,4] Hans Raskov,[1] Susanne Gjørup Sækmose,[5] Lasse Bremholm Hansen,[6] Ali Salanti,[7] Susanne Brix,[4] Ismail Gögenur[1,2]

To cite: Gögenur M, Balsevicius L, Bulut M, *et al*. Neoadjuvant intratumoral influenza vaccine treatment in patients with proficient mismatch repair colorectal cancer leads to increased tumor infiltration of CD8+ T cells and upregulation of PD-L1: a phase 1/2 clinical trial. *Journal for ImmunoTherapy of Cancer* 2023;**11**:e006774. doi:10.1136/jitc-2023-006774

► Additional supplemental material is published online only. To view, please visit the journal online (http://dx.doi.org/10.1136/jitc-2023-006774).

Accepted 26 April 2023

For numbered affiliations see end of article.

Correspondence to
Dr Mikail Gögenur;
mgog@regionsjaelland.dk

ABSTRACT

Background In colorectal cancer, the effects of immune checkpoint inhibitors are mostly limited to patients with deficient mismatch repair tumors, characterized by a high grade infiltration of CD8+T cells. Interventions aimed at increasing intratumoral CD8+T-cell infiltration in proficient mismatch repair tumors are lacking.

Methods We conducted a proof of concept phase 1/2 clinical trial, where patients with non-metastasizing sigmoid or rectal cancer, scheduled for curative intended surgery, were treated with an endoscopic intratumorally administered neoadjuvant influenza vaccine. Blood and tumor samples were collected before the injection and at the time of surgery. The primary outcome was safety of the intervention. Evaluation of pathological tumor regression grade, immunohistochemistry, flow cytometry of blood, tissue bulk transcriptional analyses, and spatial protein profiling of tumor regions were all secondary outcomes.

Results A total of 10 patients were included in the trial. Median patient age was 70 years (range 54–78), with 30% women. All patients had proficient mismatch repair Union of International Cancer Control stage I–III tumors. No endoscopic safety events occurred, with all patients undergoing curative surgery as scheduled (median 9 days after intervention). Increased CD8+T-cell tumor infiltration was evident after vaccination (median 73 vs 315 cells/mm^2, p<0.05), along with significant downregulation of messenger RNA gene expression related to neutrophils and upregulation of transcripts encoding cytotoxic functions. Spatial protein analysis showed significant local upregulation of programmed death-ligand 1 (PD-L1) (adjusted p value<0.05) and downregulation of FOXP3 (adjusted p value<0.05).

Conclusions Neoadjuvant intratumoral influenza vaccine treatment in this cohort was demonstrated to be safe and feasible, and to induce CD8+T-cell infiltration and upregulation of PD-L1 proficient mismatch repair sigmoid and rectal tumors. Definitive conclusions regarding safety and efficacy can only be made in larger cohorts.

WHAT IS ALREADY KNOWN ON THIS TOPIC

⇒ An intervention to increase T-cell infiltration in proficient mismatch repair tumors (pMMR) is needed for this major group of patients to benefit from immunotherapy.

WHAT THIS STUDY ADDS

⇒ Intratumoral administration of the seasonal influenza vaccine before curative intended colorectal cancer surgery was found to be safe, and resulted in an increased intratumoral CD8+ infiltration, a shift in gene signatures in CD8+T cells versus neutrophils, and intratumorally increased programmed death-ligand 1 protein expression and decreased FOXP3 protein expression.

HOW THIS STUDY MIGHT AFFECT RESEARCH, PRACTICE OR POLICY

⇒ The influenza vaccine is unparalleled in terms of its safety profile and is used across all patient groups and ages. If the combination of the influenza vaccine and immune checkpoint inhibitor treatment can be proven successful in future studies, the large group of patients with pMMR tumors can benefit from immune checkpoint inhibitor treatment.

Trial registration number NCT04591379.

INTRODUCTION

Colorectal cancer (CRC) is the third most diagnosed cancer and accounts for the second most deaths due to cancer.[1] The prognosis is excellent if it is diagnosed and treated while the disease is localized to the bowel wall and is worse if the tumor has regionally spread to lymph nodes. Unfortunately, many more patients tend to be diagnosed with CRC before turning 50 years of age and these patients may even have a worse prognosis.[2]

Treatment with immune checkpoints inhibitors (ICI) has led to long-term tumor regression in selected patients, and it has been demonstrated that increased intratumoral (IT) T-cell infiltration before ICI administration correlates with the probability of response to ICIs in several tumor types.[3 4] In CRC, ICIs are highly effective in deficient mismatch repair (dMMR) tumors.[5 6] Most proficient MMR (pMMR) tumors, have, unlike dMMR tumors, little-to-none IT T-cell infiltration.[7 8] Interventions to induce T-cell infiltration in pMMR tumors are thus warranted.

In preclinical models, repurposing of infectious disease vaccines have produced encouraging results in terms of increasing IT immune infiltration.[9] In a murine study, IT injection with an inactivated, non-adjuvanted seasonal influenza vaccine reduced tumor size and increased infiltration of antitumor CD8+T cells within the tumor, while application of a squalene-based adjuvanted influenza vaccine induced an increase in regulatory B cells that hindered the antitumor activity.[10] We have previously performed a registry-based cohort study that indicated that patients, who underwent curative surgery for a solid tumor and received an inactivated trivalent influenza vaccine in the postoperative period, had a decreased overall mortality and cancer-related mortality.[11] In addition, systemic influenza vaccine administration 6–12 months before surgery for CRC was associated with a reduced risk of recurrence.[12] The preclinical and epidemiological data suggest that repurposing the influenza vaccine for cancer treatment could produce encouraging results.

In this proof of concept phase 1/2 study, we aimed to investigate if neoadjuvant IT influenza vaccine treatment is safe and feasible and to explore the potential tumor microenvironment (TME) changes following the treatment.

METHODS

Patients

The study was open to all patients adhering to the following inclusion criteria: above age of 18 years, non-metastatic clinically suspected or histologically verified sigmoid or rectal adenocarcinoma, and scheduled for curative-intended surgery. The tumor needed to be described as non-obstructive at the index endoscopy and the patient cases were reviewed by a multidisciplinary team (MDT). Exclusion criteria included: intraluminal ulceration or bleeding before the intervention, ongoing immunosuppressive treatment, concurrent treatment with an investigational intervention, indication for neoadjuvant therapy, acute febrile illness, pregnancy, any previous allergic reactions to an influenza vaccine or its component, and influenza vaccine administration within 30 days of study inclusion. All study participants provided written informed consent. The study was registered at ClinicalTrials.gov.

Study design and treatment

This study was an investigator-initiated, multicenter, proof of concept, phase 1/2 clinical trial with the aim of investigating the safety and efficacy of neoadjuvant IT influenza vaccine treatment before intended curative surgery in patients with early stage sigmoid or rectal cancer. Inclusion was planned at two additional centers for a total number of 30 patients, but COVID-19 restrictions hindered this.

The study was conducted in two phases; the first phase was conducted as a pilot study including six patients. Patients were recruited from the Department of Surgery, Zealand University Hospital, after their cases were reviewed by the MDT from March to April 2021. The pilot study was conducted to ensure that no stop rules were violated.

Standard treatment involves intended curative surgery within 2 weeks after the diagnosis. Administration of the IT influenza vaccine was conducted within a few days after diagnosis and it was ensured that the experimental treatment did not lead to any significant delay in the intended curative surgery.

As the pilot study was completed without violation of any stopping rules or any serious adverse events (AEs) the second phase of the study was initiated.

The primary outcome was safety of the treatment with predefined specific stopping rules for the trial. Secondary outcomes included assessment of pathological tumor regression grade (TRG), evaluation of pathological TRG, immunohistochemistry (IHC), flow cytometry in blood, tissue bulk transcriptional analyses, spatial protein profiling of tumor regions, and any difference in the quality of recovery 15 (QoR-15) questionnaires[13] before and after the intervention.

Patients were excluded from the study if they withdrew their consent, if the disease progressed such that the patient needed another treatment, or if the investigator deemed that withdrawal was in the patient's best interest.

Intervention

Every patient received one vial (0.5 mL) of the 2021 seasonal Influvac Tetra (Viatris, USA). Influvac Tetra is a non-adjuvanted quadrivalent (subunit) influenza vaccine with inactivated fragments from four influenza viruses. A non-adjuvanted influenza vaccine was chosen based on results from the preclinical study, demonstrating that

the presence of a squalene-based adjuvant hampered the antitumor immune response.[10]

Tumors in the colon can be fibrous and rigid, restricting the possibility of injecting liquids into those parts of the tumor and with a risk of spilling part of the injection fluid into the lumen. To ensure sufficient injection volume, the vaccine was mixed with 1.5 mL saline to a total volume of 2.0 mL before administration. This mixing procedure was applied for all patients.

Included patients were scheduled for an additional endoscopy to apply the intervention. For all patients, Endoscopes GIF-H190 Olympus Exera System (Olympus, Japan) was used. Board-certified gastroenterology surgeons performed all endoscopic procedures. Before the intervention, blood samples were drawn, and a QoR-15 questionnaire was filled. During the endoscopy, the tumor was visualized and up to eight biopsies were taken, formalin fixated, and paraffin embedded (FFPE) for later analysis. After the biopsy collection, the vaccine was applied in distinct quadrants of the tumor to ensure distribution to the complete tumor area. For all patients, the vaccine was injected with a 23G, 3 mm injection needle (Jiuhong Medical Instrument, China). Any spilling of injection fluid was noted during the procedure. The patients underwent standard surgical procedures for sigmoid and rectal cancer a minimum of 7 days after the vaccine treatment, as scheduled and outlined by the MDT. On the day of admission, before surgery, blood samples were drawn, and the QoR-15 questionnaire was repeated. The surgical specimen was evaluated at the department of pathology according to the tumor, node, metastases classification and sampled for further biomarker analyses.[14]

Primary outcome

AEs and stopping rules

The primary outcome was safety of the intervention. Stopping rules were defined as perforation at the tumor site during study treatment, anaphylactic shock, and unexpected, significant or unacceptable risks to patients. Other AEs and adverse reactions were recorded from day of treatment (Day 0) until the surgery. AEs were classified according to the Common Terminology Criteria for Adverse Events V.4.0.

Secondary outcomes

TRG

All slides from the surgical specimen were evaluated by two gastrointestinal pathologists regarding TRG according to the Mandard *et al* scoring system which includes five categories with TRG1 corresponding to complete regression and TRG5 corresponding to no regression.[15]

QoR-15 questionnaire

QoR-15 is a questionnaire with 15 items that covers five different domains of recovery. To answer each item, a numerical rating of 0–10 with a composite score of 0–150 is used. Higher scores indicate better recovery, with 0–89 being rated as 'Poor'; 90–121 as 'Moderate'; 122–135 as 'Good', and 136–150 as 'Excellent'. The QoR-15 has been validated for use in Danish with a minimally clinical important difference of 8.0 points.[16 17]

IHC and digital counting of tumor-infiltrating lymphocytes

Biopsies taken at the time of vaccination that displayed presence of invasive tumor were selected for the following IHC staining. From the surgical specimen one slide with presence of both the central part of the tumor and invasive margin was selected.

Sections with a thickness of 4 µm were cut from the FFPE tissue blocks. Staining procedure is described in online supplemental materials.

Slides were scanned using a NanoZoomer S60 slide scanner (Hamamatsu, Japan). Digital images were processed using Visiopharm Quantitative Digital Pathology software (Visiopharm, Denmark, V.2021.02) and previously developed application protocol packages were used to generate automated CD3+ and CD8+ lymphocyte counts separately for the central tumor and the invasive margin. The process has been described in detail in a previously published paper.[18] We only compared tumor regions of baseline samples with central tumor regions of post vaccination samples within each individual patient.

Flow cytometry

Peripheral EDTA-anticoagulated blood samples were used to determine lymphocyte subpopulations (T, B and natural killer (NK) cells, the T cells further subdivided in CD4+ and CD8+ T cells) using the single platform method with BD Multitest 6-color TBNK kit (Becton Dickinson, California, USA) in BD TruCount tubes on FACSCanto II flow cytometers (Becton Dickinson, Belgium). Gating followed manufacturer's instructions and data analysis was performed using BD FACSDiva software V.8.0.1.

NanoString expression panels

Tissue samples from the same tissue block were used for the IHC analysis. RNA isolation and panel preparation is described in online supplemental materials. We used the used the nCounter IO360 panel of 750 endogenous human transcripts; for T-cell receptor (TCR) expression analysis—the nCounter TCR diversity panel of 119 TCR variable and constant regions and lymphocyte transcripts (NanoString, USA).

Gene expression analysis

Raw data generated with the nCounter platform was preprocessed using an iterative quality control (QC) and normalization framework as described in Bhattacharya *et al*[19] and summarized in online supplemental materials. No samples were removed after QC and normalization. Generation of principal component analysis (PCA) plots, heatmap and volcano plots are described in online supplemental materials along with description of the enrichment analysis. Differentially expressed (DE) genes between groups were identified using the Wald significance test and adjusting for multiple testing with the Benjamini-Hochberg approach.[20] Genes were considered

DE if they met threshold requirements of adjusted p value<0.05 and log2 fold change (logFC) ≥0.5. DE analysis was performed using a function from DESeq2 package (V.4.2.1) 'DESeq' with unwanted variation vectors (n=5) included in the design formula.

TCR expression analysis is described in online supplemental materials.

GeoMx digital spatial profiling

Slide preparation and sample collection

For slide preparation, FFPE tissue sections of 4 µm in thickness and 2 mm in diameter were mounted on histology slides by grouping baseline samples on one slide, and post-vaccination samples on two slides. Six to eight regions of interest (ROI) on the before and after vaccination tumor samples were chosen; one ROI from normal, highly immune-infiltrated, and low-infiltrated tumor areas from samples before vaccination; and one ROI from normal, highly immune-infiltrated tumor, low-infiltrated tumor, invasive margin with high immune cell infiltration, and low-infiltrated invasive margin areas from after vaccination samples. A specific focus in drawing ROIs in tumor and invasive margin sections was to target regions with immune infiltration guided by anti-CD45 and anti-CD8 as morphological markers. This strategy aimed to ensure that changes in protein expression were related to the intervention and not to a bias in ROI selection. A dedicated gastrointestinal pathologist drew the ROIs. This person was not blinded to the sampling time points.

The GeoMx digital spatial profiler (DSP) slide preparation user manual (MAN-10 100–03) was followed to prepare slides for data collection. For visualization of the composition of the TME, we used the following morphology markers: anti-CD45 (1:40, immune cells), anti-CD8 (1:100, T cells), anti-Pan-CK (1:40, epithelial cells), and anti-SYTO13 (1:10, DNA). All of the applied antibodies were conjugated monoclonal antibodies unless otherwise stated. A previous description of this method has been provided in Merritt *et al*.[21] We used five different panels (immune cell profiling-panel, pan-tumor-panel, cell death-panel, immune activation status-panel, immune cell typing-panel), that cover 52 antibodies and six internal reference controls.

Spatial expression data analysis

After data collection, RCC files were loaded into the GeoMx DSP analysis suite (V.2.4.2.2) where QC and scaling of data was performed (see online supplemental materials). No ROIs failed QC criteria. Following this, data was scaled to the geometric mean of the number of nuclei, and then exported to R for further analyses. The same iterative QC and normalization framework was used as for the NanoString panels.[19] We based our choice on previously published applications of this framework on GeoMx data[22–24] and assumption that unwanted variation estimation step will correct for ROI-related variation. After iterative QC and normalization, we removed n=1 vectors of unwanted variation from the data set. DE analyses were performed in R using the same packages and parameters as for NanoString expression panel analysis.

Descriptive statistics

Statistical analyses were performed using R. Summary statistics were generated based on baseline patient characteristics. To evaluate if numerical variables in all gene expression panels, GeoMx spatial profiling data, IHC data and flow data displayed normal distributions, we generated distribution histograms or QQ plots. Wald significance test was used to compute DE genes and proteins between the respective pairwise comparisons. For all other comparisons (IHC and flow data), depending on distribution, Wilcoxon rank-sum test or t-test were applied. All box plots were presented as the median and IQRs. In PCA, model group differences were assessed by permutational multivariate analysis of variance using distance matrices (PERMANOVA). In this study, p values and adjusted p values below 0.05 were considered significant unless stated otherwise. The CI for AEs was calculated as described previously.[25]

RESULTS

Patient characteristics

Ten patients were treated with the neoadjuvant IT influenza vaccine between March 10, 2021, and August 25, 2021, (see flow chart of patient inclusion in online supplemental figure S1). The study design is shown in figure 1A. All patients had pMMR tumors that were located in the sigmoid colon (n=4), mid rectum (n=2), or upper rectum (n=4). Based on pretreatment radiological assessment, patients had cT1–cT3 tumors with no distant metastases. Baseline QoR15 was 144 (range 112–150). Baseline characteristics are shown in table 1.

Patient inclusion was halted before the planned inclusion of 30 patients due to no inclusion of patients at two out of three centers as a result of COVID-19 restrictions and the expiration of the seasonal influenza vaccine (expiry date September 02, 2021) used in this trial.

Study intervention and safety

No procedural AEs were recorded for any patient. Endoscopic visualization of the quadrants (yellow arrows) of the tumor and injection of influenza vaccine are depicted in figure 1B. Endoscopic procedure time from start to end of endoscopy, including biopsy collection, and final injection of treatment was 23 min (range 10–40 min). All patients had a successful injection of the influenza vaccine suspension, but for three patients, a small, non-quantifiable, volume of the injection fluid was spilled into the lumen due to fibrous tumors.

The curative intended surgery was scheduled 9 days (range 7–13 days) from the time of treatment. In this period, one grade 1 AE (a mild fever that subsided without intervention) (10% of patients (95% CI 0 to 30). was recorded for a patient that was resolved before the scheduled surgery. The remaining patients tolerated

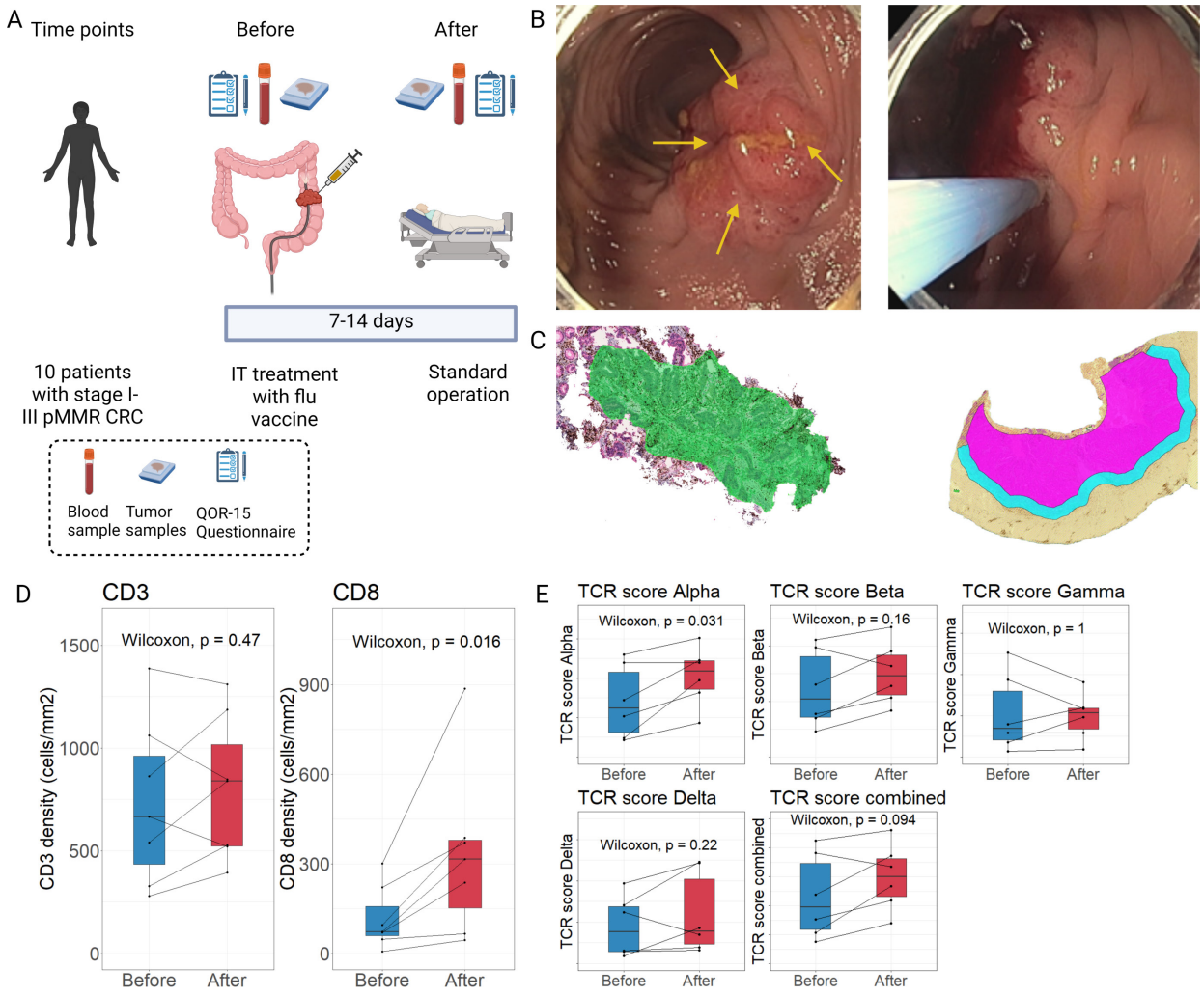

Figure 1 Neoadjuvant intratumoral influenza vaccine treatment increases CD8+T-cell infiltration and TCR alpha chain diversity. (A) Overview of the study design and sample time points. At each time point, blood and tumor samples were taken and a QoR-15 questionnaire was filled. (B) Representative pictures showing the quadrant visualization (yellow arrows, left picture) and intratumoral (IT) injection of the influenza vaccine (right picture). (C) Representative tumor tissue slides from immunohistochemistry (IHC) staining with anti-CD3/cytokeratin for digital analysis of T-cell infiltration. Tumor slides with IHC staining of anti-CD8/cytokeratin are not shown. Left picture shows a representative sample from before vaccination. Right picture shows a sample after the vaccination with the central tumor (pink) and invasive margins (light blue). (D) Comparison of the IHC staining density of CD3+ and CD8+ T cells before (green area) and after vaccination (pink area) samples (n=7). (E) Comparison of alpha, beta, gamma, and delta variable chains, and combined variable chain score between time points (n=6). (D, E) CD3+ and CD8+ T-cell densities and normalized expression of TCR variable chain expression depicted as boxplot showing median, upper and lower quartiles. Whiskers extend into a max of 1.5 times the IQR. CRC, colorectal cancer; pMMR, proficient mismatch repair; QoR-15, quality of recovery 15 questionnaire; TCR, T-cell receptor.

the treatment well, with all surgeries performed without delay. There was no significant change in QoR-15 between the day of treatment and the day of surgery (difference between groups 2.0 (95% CI −11.16 to 11.38)). All endoscopic procedural data is presented in table 2. All but one patient was deemed as Mandard TRG 5 by both pathologists, with one deemed TRG 4 by one pathologist.

Neoadjuvant IT influenza vaccine treatment increases CD8+ T-cell infiltration in pMMR tumors

In seven patients, invasive tumor tissue was present in biopsies taken before vaccination, while the biopsies from three patients only contained adenoma tissue. These three patients were therefore excluded from all tumor analyses. In figure 1C, the digital assessment of CD3+ and CD8+ T cells is depicted. When comparing before (green area, left picture in figure 1C) and after vaccination (pink area, right picture in figure 1C) tumor tissue samples, data showed no significant changes in overall density of CD3+T cells (paired Wilcoxon test, p=0.47) (figure 1D), but we found the density of the proportion of CD8+T cells to be significantly increased within the invasive tumor region after vaccination (paired Wilcoxon test, p=0.016) (figure 1D). It did not affect the results if patients previously had received a systemic influenza vaccine or if any spilling of the injection fluid occurred during the intervention (data not shown).

Table 1 Baseline characteristics of enrolled patients

Number of patients	10
Sex (%)	Female: 3 (30)
	Male: 7 (70)
Age (median (min–max))	70 (54–78)
BMI (median (min–max))	24.0 (19.6–33.1)
ASA score (%)	1: 1 (10)
	2: 6 (60)
	3: 3 (30)
WHO performance score (%)	0: 7 (70)
	1: 3 (30)
Clinical T stage	1: 1 (10%)
	2: 5 (50%)
	3: 4 (40%)
Clinical N stage	0: 9 (90%)
	1: 1 (10%)
MMR status	pMMR: 10 (100%)
QoR15 (median (min–max))	144 (112–150)
QoR15 group	Moderate: 1 (10%)
	Good: 1 (10%)
	Excellent: 8 (80%)

ASA, American Society of Anesthesiologists; BMI, body mass index; MMR, mismatch repair; QoR15, quality of recovery 15 questionnaire.

A statistically significant diversity was seen in the TCR score for alpha variable chains between the time points (paired Wilcoxon p=0.031, figure 1E). In contrast, no significant differences were seen for the remaining three variable chain types (paired Wilcoxon p>0.05, figure 1E). Combining all variable chains in one TCR score showed an increase that was not statistically significant between time points (paired Wilcoxon, p=0.094).

Genes encoding cytotoxic responses are generally enhanced within the TME following IT influenza vaccine treatment

We next investigated the expression of genes in tumor tissue excised before and after the IT influenza vaccine treatment. This was performed using the nCounter IO360 panel, comprised of 750 TME biology associated transcripts on tissue slides from before and after the vaccination. Two-dimensional data representation using PCA showed a clear difference in tumor gene expression before and after treatment (figure 2A, paired PERMANOVA: F=3.66, p=0.003). A total of 72 DE genes (logFC>0.5, adjusted p value<0.05) were identified before and after vaccination, with 27 genes being significantly upregulated and 45 genes significantly downregulated after treatment (figure 2B; distribution, correlation, p value distribution, volcano plot, and individual gene expressions plots are available in online supplemental figures S2–S5). A significantly increased expression of several cytotoxicity associated genes, such as *GZMA*, *CD8A*, *KLRB1*, and *KLRK1*, as well as the transcript encoding the co-stimulatory molecule CD27 (*CD27*) was observed. A significantly decreased expression of the genes encoding the interleukins (*IL)1B*, *IL6*, and *IL24*, the chemokines *CXCL1*, *CXCL2*, and *CXCL8* (*IL8*) and the chemokine receptor *CXCR2* was evident. The latter are all relevant for neutrophil-based immune responses. Moreover, we identified concomitantly decreased expression of transcripts encoding innate immunity associated proteins such as *CXCL5*, *CXCL6*, and *TLR1*, and importantly of transforming growth factor (*TGF)-β1*, encoding the anti-inflammatory protein TGF-β1 that is normally highly upregulated in the TME, and is one of the most critical regulators of a non-effective anticancer immunity.[26] The genes encoding cyclooxygenase 2 (*PTGS2*) and matrix metallopeptidase 1, enzymes secreted from, for example, tumor associated macrophages that increase angiogenesis through matrix degradation and endothelial cell invasion were also downregulated.[27] In the preclinical study that investigated IT influenza vaccine, a significant change in IT regulatory B cells was evident in the design that used a squalene-based adjuvanted influenza vaccine.[10] We did not find that any of the significantly expressed genes were related to regulatory B-cell function. An enrichment analysis was performed to test for cell type specific gene signature enrichment and over-representation of functional pathways between the time points that showed a disruption of neutrophil-associated pathways being affected (online supplemental file 2). Guided by the results of initial enrichment analysis, we calculated a functional enrichment score, where normalized expression of cell type and functional pathway specific genes identified or associated with the enrichment analysis as well as additional NanoString validated pathways (NS)[28] were summarized and compared (figure 2C,D). We identified that neutrophil-associated pathways were downregulated after vaccination, with significant downregulation of the Gene Ontology-based neutrophil mediated immunity and NS-neutrophils pathways (figure 2C, paired t-test, p=0.0069, and p=0.023, respectively). We found enrichment of T-cell associated pathways after vaccination (figure 2D) with significant upregulation of the NS-Th1 cell pathway and the NS-tumor-infiltrating lymphocyte

Table 2 Procedural data

Minutes from start of procedure to intratumoral influenza vaccine treatment (median (min–max))	11 (5–31)
Minutes from intratumoral influenza vaccine treatment to end of procedure (median (min–max))	9 (3–22)
Minutes from start to end of procedure (median (range))	23 (10–40)
Spilling of injection fluid	No: 7 (70%)
	Yes: 3 (30%)
Days to surgery (median (range))	9 (7–13)

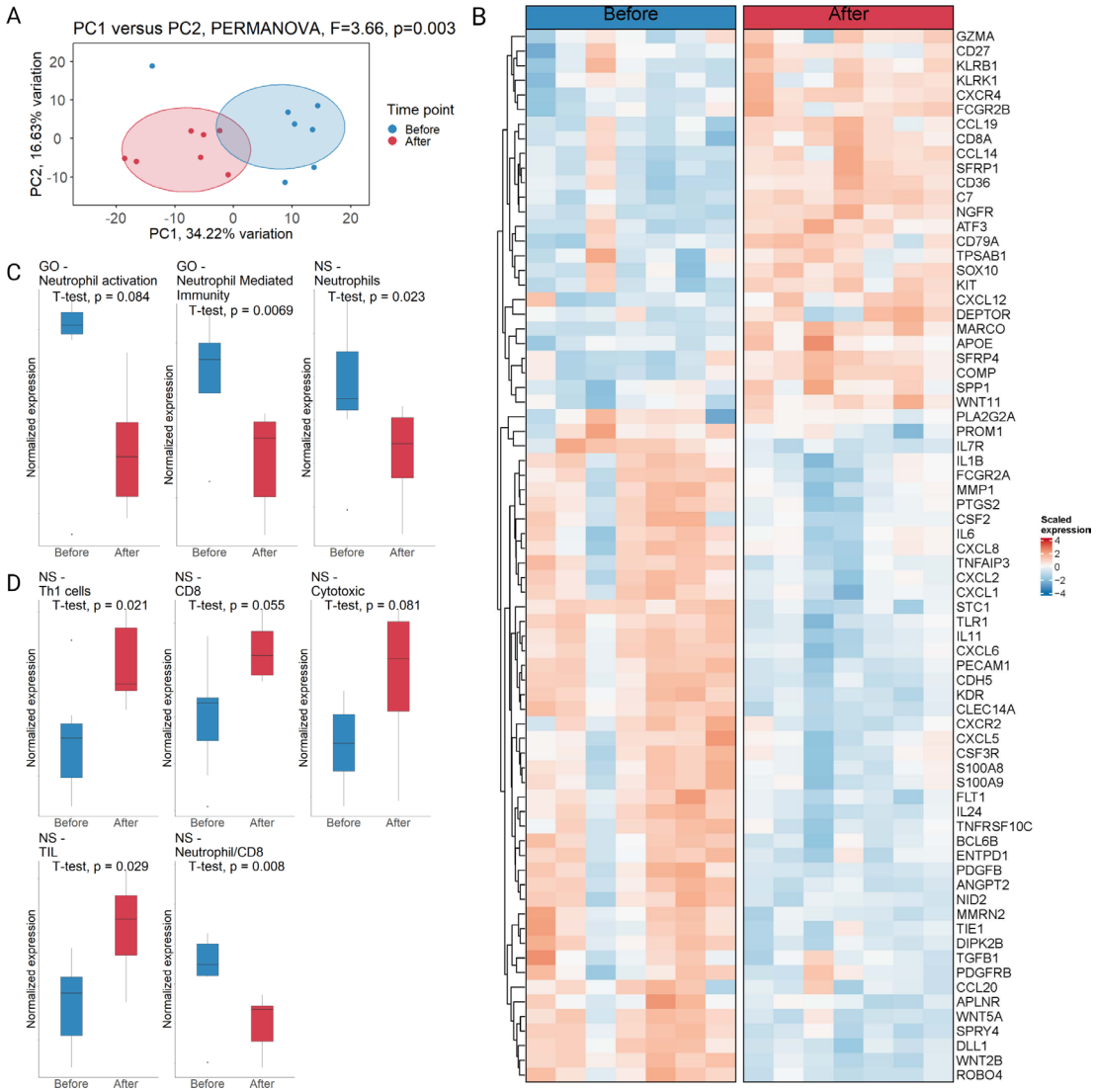

Figure 2 Changes in the tumor microenvironment after intratumoral influenza vaccine treatment. (A) Principal component analysis based on the top 400 most variable genes from nCounter IO360 panel, which includes 750 genes typically associated with tumor microenvironment biology. The statistical significance was tested using a PERMANOVA on the centroid differences between time points (n=7). (B) Heatmap of paired differentially expressed genes compared between time points (n=7, same order of patients before and after). (C, D) Significant pathways identified using functional enrichment score analysis. Here, the normalized expression of all represented genes in a pathway are analyzed via a paired t-test comparing before and after vaccination tumor samples. Normalized expression depicted as boxplot showing median, upper and lower quartiles (n=7) Whiskers extend into a max of 1.5 times the IQR. EMT, epithelial to mesenchymal transition; GO, Gene Ontology; NS, NanoString; PERMANOVA, permutational multivariate analysis of variance using distance matrices; TIL, tumor-infiltrating lymphocytes.

(TIL) pathway (paired t-test, p=0.021, and p=0.029, respectively). Importantly, we found a significant shift in the neutrophil/CD8+T-cell ratio, suggesting a shift in the immune phenotype after vaccination (paired t-test, p=0.008).

Spatial analysis of protein expression in immune-infiltrated tumor regions reveals increased local programmed death-ligand 1 and decreased FOXP3 protein expression following IT influenza vaccine treatment

To investigate the effect of IT influenza vaccine treatment on immune-infiltrated regions of tumor samples, we performed spatial protein expression analysis using the NS GeoMx platform. Representative ROIs with selection of immune-infiltrated tumor areas before and after vaccination were identified within the same patient by a gastrointestinal pathologist (figure 3A,B). A comparison of adjacent normal tissue in the samples before and after vaccination revealed no significant changes in protein expression besides the proliferation marker Ki-67 (MKI67) (online supplemental figure S6). When comparing protein expression in immune-infiltrated tumor regions before and after IT influenza vaccine treatment, we found the cellular markers programmed death-ligand 1 (PD-L1), CD3G (T cells), Human Leukocyte

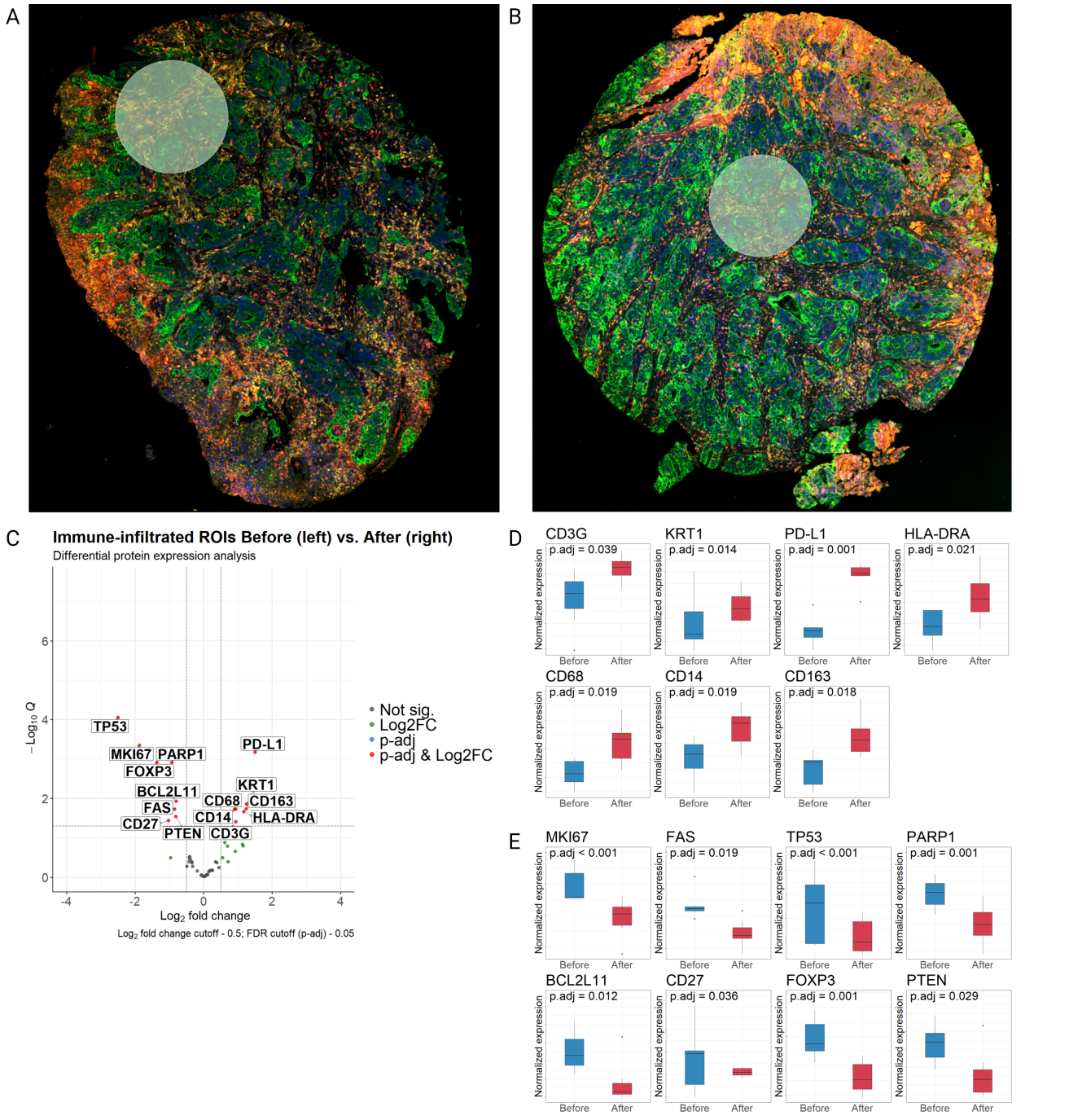

Figure 3 Spatial protein analysis within immune-infiltrated regions of tumors before and after intratumoral influenza vaccine treatment. (A, B) Picture of region of interest (ROI) selection in a patient before (A) and after (B) IT influenza vaccination. ROIs were drawn by a gastrointestinal pathologist and based on infiltration of CD45+ (yellow) and CD8+ (red) cells in areas of Pan-CK (green) and DNA (blue) positive regions. (C) Volcano plot of differentially expressed proteins in ROIs of immune-infiltrated regions of tumors before versus after vaccination (n=7). (D, E) Box plots of differentially expressed proteins upregulated (D), and downregulated (E) after vaccination (n=7). Differential expression of proteins depicted as boxplots showing median, upper and lower quartiles. Whiskers extend into a max of 1.5 times the IQR.FDR: False Discovery Rate; HLA-DRA, Human Leukocyte Antigen DR alpha chain; IT, intratumoral; KRT1, keratin 1; logFC, log2 fold change; MKI67, marker Ki-67; PD-L1, programmed death-ligand 1.

Antigen DR alpha chain (HLA-DRA, antigen presenting cells), and keratin 1 to be significantly upregulated (logFC>0.5, adjusted p value<0.05) after treatment, along with the monocyte and macrophage markers CD14, CD68, and CD163 (figure 3C,D). We found FOXP3, the transcriptional regulator of regulatory T cells (Tregs), a cell type, that is, typically abundant in TME, to be down-regulated on treatment (figure 3E). The DNA-repair proteins and tumor suppressors TP53, PTEN, and PARP1 were likewise significantly downregulated, along with

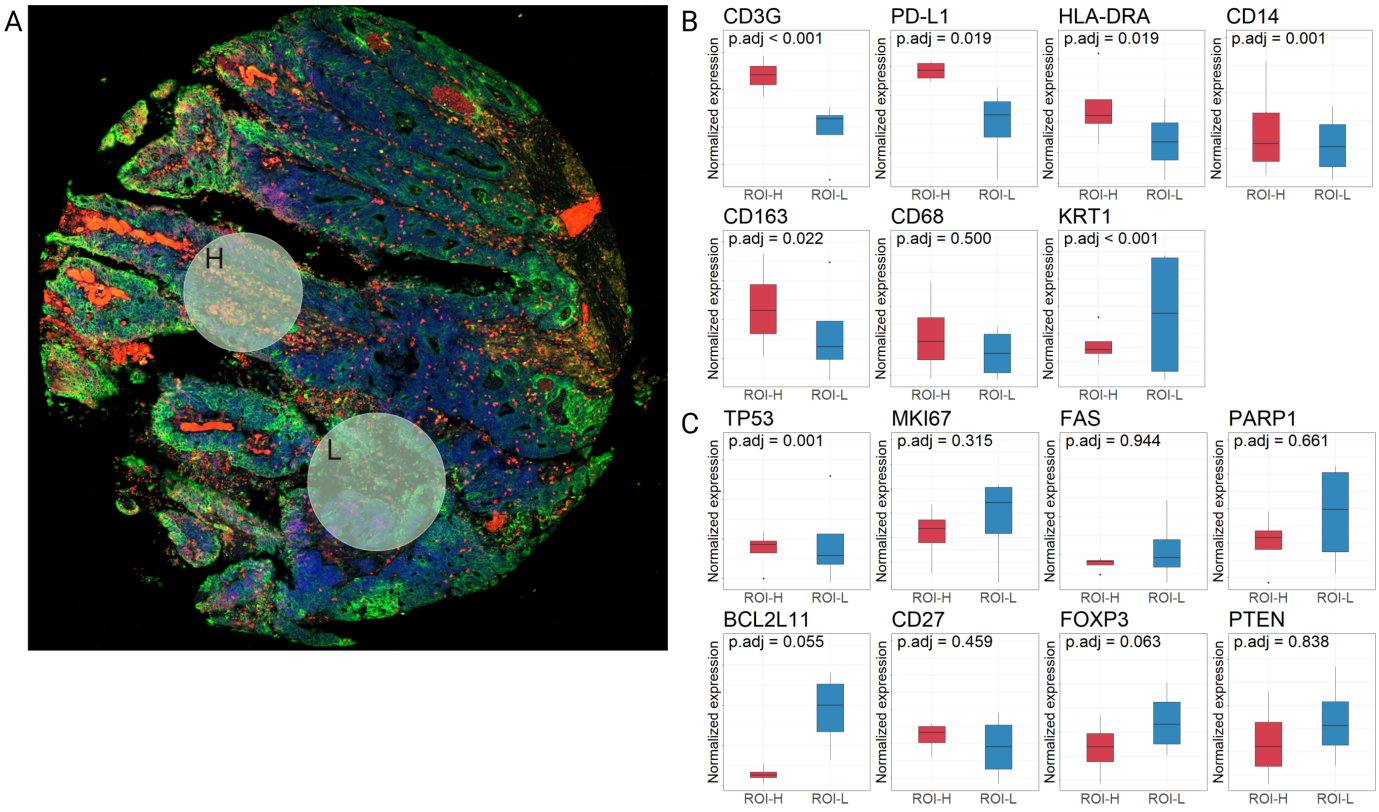

Figure 4 Spatial analysis of high immune-infiltrated versus low immune-infiltrated regions of tumors after vaccination. (A) Pictures of region of interest (ROI) selection in a patient after vaccination. Upper ROI designates a tumor area with high immune-infiltration (ROI-H) while the lower ROI designates a tumor area with low immune-infiltration (ROI-L). (B) Box plots of differentially expressed (DE) proteins upregulated on vaccination (from figure 3 (n=4)). (C) Box plots of the downregulated DE proteins on vaccination (from figure 3 (n=4)). Differential expression of proteins depicted as boxplots showing median, upper and lower quartiles. Whiskers extend into a max of 1.5 times the IQR. HLA-DRA, Human Leukocyte Antigen DR alpha chain; KRT1, keratin 1; MKI67, marker Ki-67; PD-L1, programmed death-ligand 1.

the proliferation MKI67, and the apoptosis-regulating proteins FAS (CD95) and BCL2L11. The co-stimulatory molecule CD27 was found to be downregulated at the protein level within the immune-infiltrated tumor regions (figure 3E), while being upregulated at protein level across the general tumor tissue that may also contain normal tissue (figure 2B). No significant difference in the B-cell marker CD20 was found.

Spatial analysis of protein expression in high immune-infiltrated versus low immune-infiltrated regions of tumors after vaccination

When comparing paired samples of high immune-infiltrated and low immune-infiltrated tumor areas from the same patients after vaccination (representative ROIs in figure 4A), we identified that PD-L1, CD3G and HLA-DRA protein expression were significantly upregulated (logFC>0.05, adjusted p value<0.05) in the high immune-infiltrated ROIs (ROI-H) compared with the low immune-infiltrated ROIs (ROI-L), suggesting that PD-L1 protein expression in the tumor cells is linked to presence of immune cells (figure 4B). There was no difference in CD68 expression, while CD163 and CD14 upregulation were seen in ROI-H only. FOXP3 expression did not differ significantly between ROI-H and ROI-L (figure 4C). Only TP53 remained downregulated in high immune-infiltrated tumor ROIs compared with low immune-infiltrated tumor ROIs.

No changes in the circulating levels of CD8+ T cells and C-reactive protein but enhanced systemic B-cell levels on IT influenza vaccination

Despite the change in tumor-infiltrating CD8+T cells in the invasive region of tumors on IT influenza vaccination (figure 1D), we identified no increases in systemic levels of general CD3+T cells nor in CD8+T cells in circulating blood (figure 5A,B). This lack of difference was also the case for general leukocytes, lymphocytes, neutrophils, thrombocytes, CD4+T cells, the ratio between CD8+ and CD4+ cells, CD56+cells (NK cells), and for the acute phase protein C-reactive protein. However, we noticed a significant increase in circulating CD19+cells (B cells) on IT influenza vaccination (p=0.024).

DISCUSSION

In the present study, we show that neoadjuvant IT influenza vaccine treatment is a safe intervention in patients with pMMR early stage CRC, causing no delay of surgery, and that it increases the CD8+T-cell infiltration of the

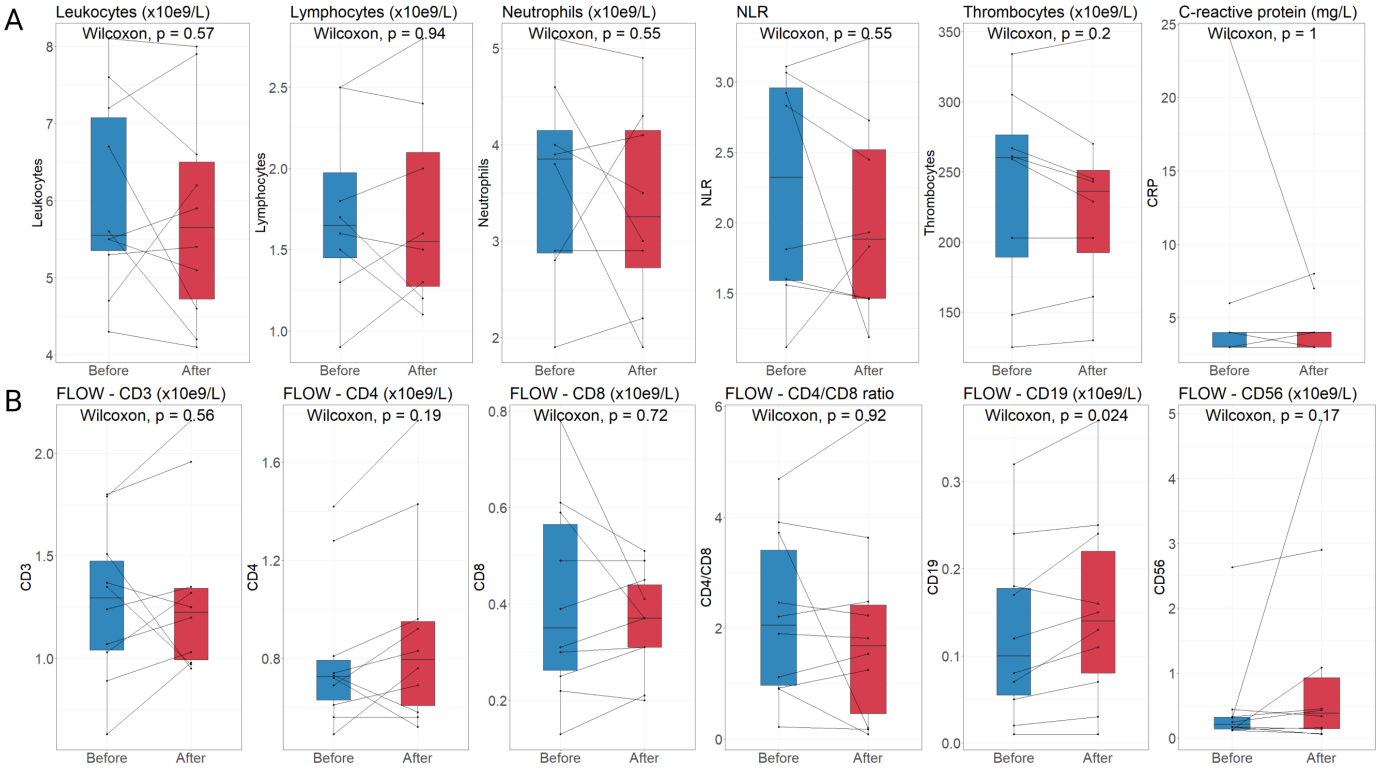

Figure 5 Circulating levels of immune cells and C-reactive protein after vaccination. (A) Overview of general immune cell populations (leukocytes (n=10), lymphocytes (n=8), neutrophils (n=8), neutrophils/lymphocytes ratio (n=8), and thrombocytes (n=8)), and the concentration of C-reactive protein (CRP, n=9). (B) Overview of flow cytometry analyses to determine subpopulations (CD3+T cells, CD4+T cells, CD8+T cells, B cells (CD19+), and natural killer cells (CD56+), all n=10). Concentration of immune cells and CRP depicted as boxplots showing median, upper and lower quartiles. Whiskers extend into a max of 1.5 times the IQR.

tumor when investigated within a median of 9 days after the intervention. A downregulation of FOXP3, which is mainly expressed by Tregs in the TME, and of innate immune pathways involving neutrophils was evident along with a local upregulation of PD-L1 protein expression after vaccination.

Neoadjuvant immunotherapy is a mainstay in several cancer types, with recent studies showing 100% pathological response in dMMR CRC.[5 6] However, response rates in pMMR CRC are limited.[5] A major difference between the pMMR and dMMR phenotypes is the level of immune cell infiltration of especially CD8+T cells, with pMMR tumors commonly reported with a low level of infiltration. Several studies have shown that pretreatment levels of CD8+T-cell infiltration are central for a robust response to ICI treatment.[29 30] However, interventions that lead to increased infiltration of CD8+T cells are lacking.

Our results show that repurposing the seasonal influenza vaccine increases the density of CD8+T cells and PD-L1 protein expression in pMMR tumors, which may be translated to a possible benefit of ICI treatment that targets either PD-L1 on tumor cells or its ligand programmed cell death protein-1 on T cells to downregulate their immunosuppressive effects and improve the tumor-killing effect of CD8+T cells. Importantly, this analysis was done in comparison of only tumor regions before and after vaccination, without including the invasive margin. The increase in the proportion of CD8+T cells in tumor areas is in line with preclinical data on IT influenza vaccine treatment.[10] The TCR repertoire diversity score for alpha chain variants also increased within the tumor suggesting that the infiltrating CD8+T cells are more diverse and may have been presented for neoantigens. However, we cannot determine based on the current investigations if the neoantigens stem from the vaccine or the cancer cells, but due to upregulation of PD-L1 on post-vaccination tumor cells there is an indication that at least some of the CD8+T cells are able to interact with the tumor.[31] Regardless of their specificity, the increased density of CD8+T cells indicate that the intervention has induced a change to a more 'hot' phenotype of the TME.

Along with the influx of CD8+T cells, we see a distinct change in messenger RNA expression in the TME with a change in key cytotoxic genes. The functional enrichment analysis revealed a significant upregulation of the NS validated TH1 cell and TIL pathways.[28] Several innate immunity genes were significantly downregulated, along with a significant downregulation of several neutrophil-associated pathways. Indeed, a significant increase in the CD8+T cell to neutrophil ratio suggests a shift towards a more antitumor immune phenotype.

Finally, we were interested in treatment-induced changes in specific regions of the tumors before and after vaccination. The above-mentioned results were found

using common strategies where bulk tissues are investigated, including both normal stroma, invasive margin, and tumor regions. In order to investigate isolated changes within immune-infiltrated tumor regions we applied spatial protein expression analysis and found a striking significant difference in upregulation of PD-L1 and downregulation of FOXP3 after vaccination. The upregulation of PD-L1 is crucial as it is a biomarker of ICI efficacy demonstrated in several studies.[29 32] Indeed, the preclinical data from mice suggested a synergistic effect of combining IT influenza vaccine treatment with ICI.[10] Together with the increased CD8+T-cell infiltration, the upregulation of PD-L1 suggests that the pMMR tumors have been primed by the IT influenza vaccine treatment to respond to ICI treatment. Baseline levels of FOXP3, a marker of the immunosuppressive Treg type, have also been shown to influence the efficacy of ICI treatment, with lower levels of FOXP3 seen in responding patients.[33] This further adds to the notion that IT influenza vaccine treatment may prime the pMMR tumors for ICI treatment. The spatial protein analysis showed an increased expression of the macrophage markers CD14, CD68 and CD163 in immune-infiltrated tumor areas after IT influenza vaccine treatment. It has earlier been suggested based on in vitro studies that CD163 may represent an M2-like macrophage marker, but newer data using in situ IHC indicates that CD163 may not be a specific marker for M2-like macrophages since the numbers of CD163+macrophages were found to be higher in TME of cases with a cytotoxic/Th1 signature.[34] These macrophage markers were increased along with HLA-DRA for presentation of antigenic peptides for CD4+T cells. Among these three macrophage markers, we identified that CD14 and CD163 were selectively enriched within high immune-infiltrated versus low immune-infiltrated tumor regions on vaccination, thus pointing to selective macrophage markers being expressed by macrophages within immune-infiltrating regions. The spatial GeoMx method does not allow for identification of double-positive or triple-positive cells that may otherwise have resulted in a more specific identification of, for example, M1-like polarization over M2-like's within the tumor tissue. Moreover, a concomitant downregulation of three DNA repair proteins and tumor suppressors TP53, PTEN, and PARP1 along with the proliferation MKI67 and the pro-apoptotic proteins FAS and BCL2L11 was observed. This suggests an interesting switch in the tumor cells with less proliferation along with less apoptosis and DNA repair. Finally, we noted a significant downregulation of CD27 at protein level in tumor-infiltrated regions, but not at transcript level within the general tumor tissue, which may also contain normal tissue areas. CD27 is a protein involved at different time points in the differentiation of T cells.[35] The expression is downregulated during differentiation and upregulated in memory T cells, while a persistent upregulation can be seen in FOXP3+Tregs. A reduced CD27 protein expression may thus align with our findings of reduced FOXP3 levels in immune-infiltrated tumor areas. Altogether, the non-proliferative, less apoptotic tumor phenotype combined with increased cytotoxic potential, decreased FOXP3 levels, and increased PD-L1 in immune-infiltrated tumor regions point to induction of an antitumor signature by IT influenza vaccine treatment. Finally, in the preclinical IT influenza vaccine study, a significant role of regulatory B cells were evident in abrogating the antitumor response if the influenza vaccine included a squalene-based adjuvant when compared with the non-adjuvanted version.[10] In our data, we saw no significant changes on the transcript or protein level of regulatory B cells, which was expected as we used a non-adjuvanted influenza vaccine in the study.

A limitation of our study is the inclusion of a low number of patients which was due to expiration of the used influenza vaccine and restricted patient inclusion during COVID-19. The study coordinators deemed that using another influenza vaccine in the same study would convolute the results, and patient inclusion was therefore halted. Further, the 9 days between treatment and surgery may hamper appearance of activated tumor-specific T cells in the tumor tissue, as well as in the circulation, as the expansion of activated clones, and their appearance in the tumor may require at least 14–21 days due to the division rates of T cells on activation (ca. one cell division per day). The short period was due to a requirement from the ethics committee to adhere to the Danish cancer care regulations dictating that surgery needs to be performed within 14 days after diagnosis. The short period could also explain the limited pathological response. As the potential safety and effects of the IT influenza vaccine treatment have been illuminated in the present study, future studies should extend the period from IT influenza vaccine treatment to surgery to allow for increased time for activation and proliferation of tumor-specific CD8+T cells, and consider to investigate the intervention in a randomized setting.

Compared with the recent discovery of neoadjuvant chemoradiation as a means to induce a cytotoxic TME,[36] the influenza vaccine is unparalleled in terms of a favorable safety profile, and its wide usage in patients with cancer across age and frailty.[37] Furthermore, the influence of previous influenza vaccination was minimal across our analyses, encouraging its prospects. As indicated in the preclinical data and further substantiated by the present study, future studies should combine IT influenza vaccine treatment with ICI in a study design that allows a prolonged time from intervention to surgery. The prolonged time would ensure sufficient recruitment and differentiation of T cells and the potential for a pathological response that reduces the tumor size.

Based on our present study, we can conclude that neoadjuvant IT influenza vaccine treatment is a safe intervention that induces an increased infiltration of CD8+T cells in the pMMR TME, a shift in gene signatures related to CD8+T cells versus neutrophils, with downregulated FOXP3 levels, and enhanced PD-L1 protein expression that may prime pMMR tumors to be susceptible to

ICI treatment. Further studies should investigate a more extended period from the IT influenza vaccine to surgery and combine it with ICI treatment.

Author affiliations
[1]Center for Surgical Science, Department of Surgery, Zealand University Hospital Koge, Koge, Denmark
[2]Department of Clinical Medicine, University of Copenhagen, Kobenhavn, Denmark
[3]Department of Pathology, Zealand University Hospital Roskilde, Roskilde, Denmark
[4]Department of Biotechnology and Biomedicine, Technical University of Denmark, Lyngby, Denmark
[5]Department of Clinical Immunology, Zealand University Hospital Koge, Koege, Denmark
[6]Department of Surgery, Zealand University Hospital Koge, Koge, Denmark
[7]Department of Infectious Diseases, Copenhagen University Hospital, Kobenhavn, Denmark

Twitter Mikail Gögenur @MGogenur and Susanne Brix @BrixSusanne

Acknowledgements The authors acknowledge Peter Johan Heiberg Engel for his contributions to region of interest selection for the GeoMx digital spatial profiling, and Michael Bzorek for immunohistochemistry sample preparation. Biorender.com was used for all figure preparation. The authors thank the patients who volunteered to participate in the study, and their families; physicians and nurses who cared for patients and supported this clinical trial.

Contributors Conceptualization: MG, IG. Methodology: MG, IG, AS. Software: MG, LB. Formal analysis: MG, LB. Data Curation: MG, LB, A-MKF. Writing—Original Draft: MG. Writing—Review and Editing: All authors. Visualization: MG, LB. Supervision: IG, AS, SB. Guarantor: IG

Funding This study was funded by the Aage and Johanne Louis-Hansen foundation (grant nr. 21-2B-8305 / L 276), Axel Muusfeldt foundation (grant nr. 2021-0250), and the Else and Mogens Wedell-Wedellborgs Foundation (grant nr. 1-22-1).

Competing interests None declared.

Patient consent for publication Consent obtained directly from patient(s).

Ethics approval The study was approved by the Danish Regional Committee on Health Research Ethics (approval number SJ-834) and by the Danish Medicines Agency (approval number 2020041760). It was monitored by the Good Clinical Practice unit (Bispebjerg and Frederiksberg Hospital, University of Copenhagen) as required by Danish law. Participants gave informed consent to participate in the study before taking part.

Provenance and peer review Not commissioned; externally peer reviewed.

Data availability statement Data are available upon reasonable request.

ORCID iD
Mikail Gögenur http://orcid.org/0000-0001-7768-324X

REFERENCES

1 Sung H, Ferlay J, Siegel RL, *et al*. Global cancer statistics 2020: GLOBOCAN estimates of incidence and mortality worldwide for 36 cancers in 185 countries. *CA Cancer J Clin* 2021;71:209–49.
2 Mauri G, Sartore-Bianchi A, Russo A-G, *et al*. Early-Onset colorectal cancer in young individuals. *Mol Oncol* 2019;13:109–31.
3 Tumeh PC, Harview CL, Yearley JH, *et al*. Pd-1 blockade induces responses by inhibiting adaptive immune resistance. *Nature* 2014;515:568–71.
4 Taube JM, Klein A, Brahmer JR, *et al*. Association of PD-1, PD-1 ligands, and other features of the tumor immune microenvironment with response to anti-PD-1 therapy. *Clin Cancer Res* 2014;20:5064–74.
5 Chalabi M, Fanchi LF, Dijkstra KK, *et al*. Neoadjuvant immunotherapy leads to pathological responses in MMR-proficient and MMR-deficient early-stage colon cancers. *Nat Med* 2020;26:566–76.
6 Cercek A, Diaz LA. Pd-1 blockade in mismatch repair-deficient rectal cancer. reply. *N Engl J Med* 2022;387:855–6.
7 Maby P, Tougeron D, Hamieh M, *et al*. Correlation between density of CD8+ T-cell infiltrate in microsatellite unstable colorectal cancers and frameshift mutations: a rationale for personalized immunotherapy. *Cancer Res* 2015;75:3446–55.
8 Fabrizio DA, George TJ, Dunne RF, *et al*. Beyond microsatellite testing: assessment of tumor mutational burden identifies subsets of colorectal cancer who may respond to immune checkpoint inhibition. *J Gastrointest Oncol* 2018;9:610–7.
9 Vandeborne L, Pantziarka P, Van Nuffel AMT, *et al*. Repurposing infectious diseases vaccines against cancer. *Front Oncol* 2021;11:688755.
10 Newman JH, Chesson CB, Herzog NL, *et al*. Intratumoral injection of the seasonal flu shot converts immunologically cold tumors to hot and serves as an immunotherapy for cancer. *Proc Natl Acad Sci U S A* 2020;117:1119–28.
11 Gögenur M, Fransgård T, Krause TG, *et al*. Association of postoperative influenza vaccine on overall mortality in patients undergoing curative surgery for solid tumors. *Int J Cancer* 2021;148:1821–7.
12 Gögenur M, Fransgård T, Krause TG, *et al*. Association of influenza vaccine and risk of recurrence in patients undergoing curative surgery for colorectal cancer. *Acta Oncol* 2021;60:1507–12.
13 Stark PA, Myles PS, Burke JA. Development and psychometric evaluation of a postoperative quality of recovery score: the qor-15. *Anesthesiology* 2013;118:1332–40.
14 Nagtegaal ID, Odze RD, Klimstra D, *et al*. The 2019 who classification of tumours of the digestive system. *Histopathology* 2020;76:182–8.
15 Mandard AM, Dalibard F, Mandard JC, *et al*. Pathologic assessment of tumor regression after preoperative chemoradiotherapy of esophageal carcinoma. clinicopathologic correlations. *Cancer* 1994;73:2680–6.
16 Kleif J, Edwards HM, Sort R, *et al*. Translation and validation of the Danish version of the postoperative quality of recovery score qor-15. *Acta Anaesthesiol Scand* 2015;59:912–20.
17 Myles PS, Myles DB, Galagher W, *et al*. Minimal clinically important difference for three quality of recovery scales. *Anesthesiology* 2016;125:39–45.
18 Fiehn A-MK, Reiss B, Gögenur M, *et al*. Development of a fully automated method to obtain reproducible lymphocyte counts in patients with colorectal cancer. *Appl Immunohistochem Mol Morphol* 2022;30:493–500.
19 Bhattacharya A, Hamilton AM, Furberg H, *et al*. An approach for normalization and quality control for nanostring RNA expression data. *Brief Bioinform* 2021;22:bbaa163.
20 Benjamini Y, Hochberg Y. Controlling the false discovery rate: a practical and powerful approach to multiple testing. *Journal of the Royal Statistical Society: Series B (Methodological)* 1995;57:289–300.
21 Merritt CR, Ong GT, Church SE, *et al*. Multiplex digital spatial profiling of proteins and RNA in fixed tissue. *Nat Biotechnol* 2020;38:586–99.
22 Stewart RL, Matynia AP, Factor RE, *et al*. Spatially-resolved quantification of proteins in triple negative breast cancers reveals differences in the immune microenvironment associated with prognosis. *Sci Rep* 2020;10:6598.
23 Lee MH, Perl DP, Steiner J, *et al*. Neurovascular injury with complement activation and inflammation in covid-19. *Brain* 2022;145:2555–68.
24 Kulasinghe A, Monkman J, Shah ET, *et al*. Spatial profiling identifies prognostic features of response to adjuvant therapy in triple negative breast cancer (TNBC). *Front Oncol* 2021;11:798296.
25 Simon S. Confidence interval with zero events. 2001. Available: http://new.pmean.com/zero-events/
26 Roberts AB, Wakefield LM. The two faces of transforming growth factor beta in carcinogenesis. *Proc Natl Acad Sci U S A* 2003;100:8621–3.
27 Klimp AH, Hollema H, Kempinga C, *et al*. Expression of cyclooxygenase-2 and inducible nitric oxide synthase in human

ovarian tumors and tumor-associated macrophages. *Cancer Res* 2001;61:7305–9.
28 Danaher P, Warren S, Dennis L, *et al*. Gene expression markers of tumor infiltrating leukocytes. *J Immunother Cancer* 2017;5:18.
29 Ferrarotto R, Amit M, Nagarajan P, *et al*. Pilot phase II trial of neoadjuvant immunotherapy in locoregionally advanced, resectable cutaneous squamous cell carcinoma of the head and neck. *Clin Cancer Res* 2021;27:4557–65.
30 Amaria RN, Reddy SM, Tawbi HA, *et al*. Neoadjuvant immune checkpoint blockade in high-risk resectable melanoma. *Nat Med* 2018;24:1649–54.
31 Buchbinder EI, Desai A. Ctla-4 and PD-1 pathways: similarities, differences, and implications of their inhibition. *Am J Clin Oncol* 2016;39:98–106.
32 Cortes J, Cescon DW, Rugo HS, *et al*. Pembrolizumab plus chemotherapy versus placebo plus chemotherapy for previously untreated locally recurrent inoperable or metastatic triple-negative breast cancer (keynote-355): a randomised, placebo-controlled, double-blind, phase 3 clinical trial. *Lancet* 2020;396:1817–28.
33 Shui IM, Liu XQ, Zhao Q, *et al*. Baseline and post-treatment biomarkers of resistance to anti-PD-1 therapy in acral and mucosal melanoma: an observational study. *J Immunother Cancer* 2022;10:e004879.
34 Barros MHM, Hassan R, Niedobitek G. Tumor-Associated macrophages in pediatric classical Hodgkin lymphoma: association with Epstein-Barr virus, lymphocyte subsets, and prognostic impact. *Clinical Cancer Research* 2012;18:3762–71.
35 van Lier RA, Borst J, Vroom TM, *et al*. Tissue distribution and biochemical and functional properties of tp55 (CD27), a novel T cell differentiation antigen. *J Immunol* 1987;139:1589–96.
36 Lauret Marie Joseph E, Kirilovsky A, Lecoester B, *et al*. Chemoradiation triggers antitumor Th1 and tissue resident memory-polarized immune responses to improve immune checkpoint inhibitors therapy. *J Immunother Cancer* 2021;9:e002256.
37 Wumkes ML, van der Velden AMT, Los M, *et al*. Serum antibody response to influenza virus vaccination during chemotherapy treatment in adult patients with solid tumours. *Vaccine* 2013;31:6177–84.